Report Title: **Single Crystal Sapphire Optical Fiber Sensor Instrumentation**

Type of Report: **Semi-Annual Report**

Report Period Start Date: **April 1, 2000**

Report Period End Date: **September 30, 2000**

Principle Investigators: **Dr. Anbo Wang, Dr. Russell May, Dr. Gary R. Pickrell**

Date Report was issued: **October 28, 2000**

DOE Award Number: **DE-FC26-99FT40685**

Name and Address of Submitting Organization:

Virginia Tech.

340 Whittemore Hall

Blacksburg, Virginia 24061

Introduction

The goal of this 30 month program is to develop reliable accurate temperature sensors based on single crystal sapphire materials that can withstand the temperatures and corrosive agents present within the gasifier environment. The research for this reporting period has been segregated into two parallel paths – corrosion resistance measurements for single crystal sapphire fibers and investigation of single crystal sapphire sensor configurations. The ultimate goal of this phase one segment is to design, develop and demonstrate on a laboratory scale a suitable temperature measurement device that can be field tested in phase two of the program.

SECTION I. Design of the Sapphire Based Temperature Sensor

1. Principle Of Operation of the Birefringence Based Sapphire Sensor Configuration

Sapphire, because of the symmetry of the atomic arrangements in the structural units for the single crystal sapphire fibers, exhibits differences in the speed of propagation of light along different crystallographic axis. This difference in the speed of propagation of light with respect to the different crystallographic axis is termed birefringence. Since the electron probability density distribution is related to the spacing between adjacently "bonded" atoms, and since the propagation speed of light in a particular direction in a crystal is a function of the electron density distribution, as the spacing between atoms changes the speed of light propagation changes. Since the thermal expansion coefficients of sapphire are different along the a and c crystallographic directions, the change in spacing between adjacent atoms in each of these directions will be different for a given temperature change. This suggests that the magnitude of the birefringence of the single crystal sapphire fiber will change with temperature.

2.1 Polarization Based Measurement Technique

Polarization is a fundamental property of light, which like amplitude, frequency and phase can be used to measure changes in the state of a system. The determination of the state of polarization in a system can provide information about photochemical or photo-biological or physical processes, which are difficult or impossible to be obtained by spectral studies in which light polarization is not controlled and monitored. Techniques employing polarized light are already widely adopted in spectroscopic techniques to provide different types of information about atoms or molecules, like the electronic structure of the molecules, or orientation of the molecule.

Light is composed of an oscillating electromagnetic field and is made up of an oscillating electric field and an oscillating magnetic field with the same frequency but orientated perpendicular to the electric field. For detection schemes which are only sensitive to electric field, we can ignore the effect of the magnetic field. Therefore, we can consider

light as an electric field whose magnitude oscillates in time and that, for linearly polarized light, is oriented along the polarization axis of the light. From the electric field shown in Figure 1with the light propagating along the z axis, the linearly polarized light along the x axis can be described by equation (1):

$$E(z,t) = E_x^0 \sin(2pgt - 2pz/l + f_0) \quad (1)$$

where g is the frequency of the light wave, l is its wavelength, E_x^0 is the maximum amplitude, and f_0 is phase.

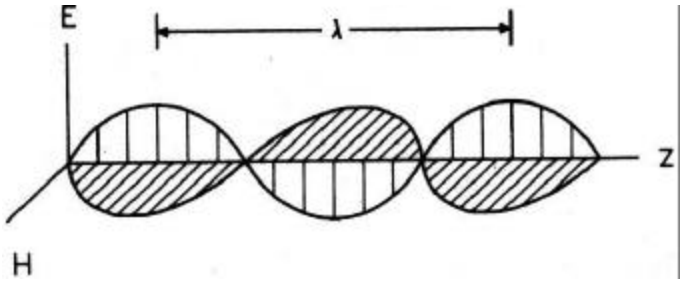

Figure 1. Schematic Representation Of A Propagating Lightwave Showing The Oscillatory Nature Of Orthogonal Electric And Magnetic Field Vectors

Linearly polarized light with its polarization axis oriented in any direction in the xy plane can be thought of as consisting of two components oriented along the x and y axes respectively, i.e., E_x and E_y. where E_x and E_y have identical magnitudes but oscillate 90^0 out of phase. This will form circularly polarized light, as shown in Figure 2.

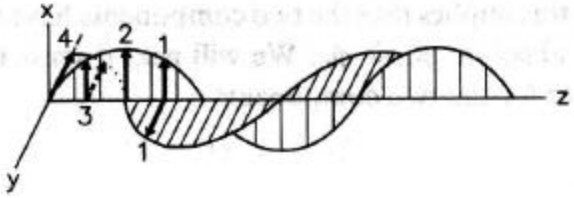

(a)

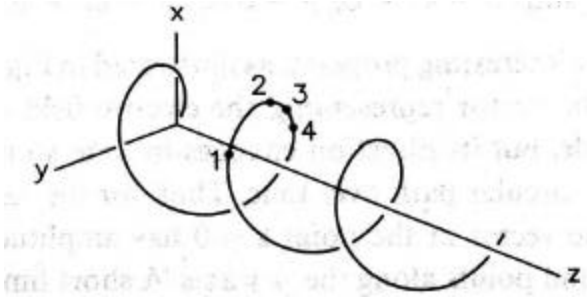

(b)

Figure 2. Representation Of Circularly Polarized Light.(A) Orthogonal Linear Components With Equal Amplitude And 90^0 Relative Phase Shift; (B) Path At A Single Instant In Time Of The Resultant Electric Field Vector Represented In (A).

In the more general case, when E_x and E_y have different magnitudes and oscillate at an arbitrary phase with respect to each other, they form elliptically polarized light, as shown in Figure 3.

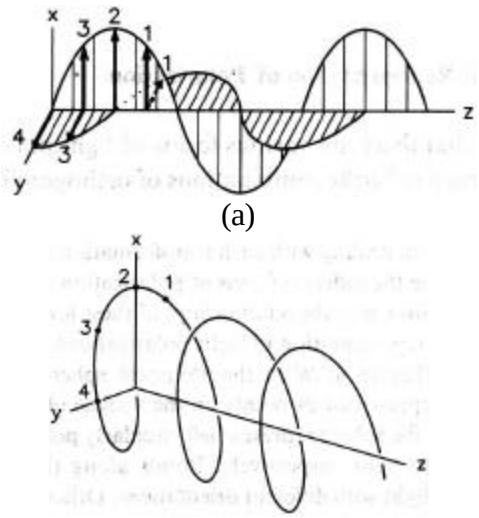

Figure 3. Representation of elliptically polarized light.(a) orthogonal linear components with unequal amplitude and arbitrary relative phase shift; (b) path at a single instant in time of the resultant electric field vector represented in (a).

However, our eyes are polarization-insensitive, so we can only use some physical components, such as linear polarizers, retarders, depolarizers, etc., to manipulate polarized light transmission. In our experimental setup we employ a birefringent retarder in the design of our sensing system as will be discussed in detail.

Retarders allow the phase of two orthogonal polarization components of light to be varied with respect to one another. A common example of a retarder is the quarter-wave plate, which increases the phase of one linear polarization by 90^0 relative to the other.

Retardation is a result of differences in refractive index as a function of crystallographic direction. As light passes from a vacuum into a material body, the speed of light is reduced by a factor that is the reciprocal of the refractive index. If a body retards all polarizations to the same degree, independent of the propagation direction, the body is said to be isotropic. On the other hand, if the refractive index depends on the polarization form and direction of propagation, the body is said to be anisotropic. In general, an anisotropic material is completely characterized by three principal refractive indices that can be represented in an index ellipsoid. Those crystals in which one principal refractive index is different from the other two are called uniaxial. In uniaxial materials, the rays that are used to define the unique (optic) axis are called extraordinary rays, with a refractive index termed n_e, and those that are associated with the other axes are called ordinary rays, with refractive index n_o. Those crystals in which all three principal refractive indices are different are called biaxial. Bodies with different principal refractive indices are also said to be birefringent. Sapphire is a uniaxial crystal because of its hexagonal crystalline structure.

A more common use of birefringent materials is in linear retarders. They are used to introduce a phase difference between two linear polarizations of light. In uniaxial

crystals, the orientation of the polarization whose phase changes the most within the retarder defines the slow axis of the retarder, with its refractive index being defined as n_o. The principal optical axis defines the fast axis of the retarder, with its refractive index being defined as n_e. The measure of performance for retarders is the retardance or extra phase angle induced by propagation of the light along these two different axes. Sapphire not only possess superior high temperature properties, but also is a birefringent material, so that it can be used as a phase retarding material at high temperatures. Single crstal sapphire is a negative crystal ($n_e<n_o$). For a wavelength of 589nm, n_o=1.768, and n_e=1.760, yielding a birefringence of 0.008. The xy plane of the index ellipsoid of single crystal sapphire is shown as Figure 4.

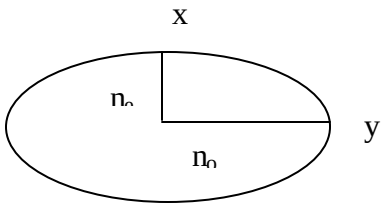

Figure 4. The XY Plane Of The Index Ellipsoid Of Single Crystal Sapphire

As linearly polarized light passes through one sapphire flat, corresponding to Figure 4, the light can be divided along the x and y directions separately. Along the x axis the refractive index will be n_e, along the y axis the refractive index will be n_o. As shown in Figure 5, at the input surface of the sapphire flat, the ordinary ray and exrodinary ray are still in phase, i.e phase difference Δj =0. After the light passes through the flat, the phase difference d will change from zero to

$$d = 2pd\Delta n / l \ , \qquad (2)$$

where d is the thickness of sapphire flat, $\Delta n = n_o - n_e = 0.008$, $l = 632.8nm$ (for helium neon laser light). Depending on the magnitude of d and the alignment angle θ between the input light polarization direction and the flat principal axes directions, the output light can be linearly polarized, circularly polarized or elliptically polarized light.

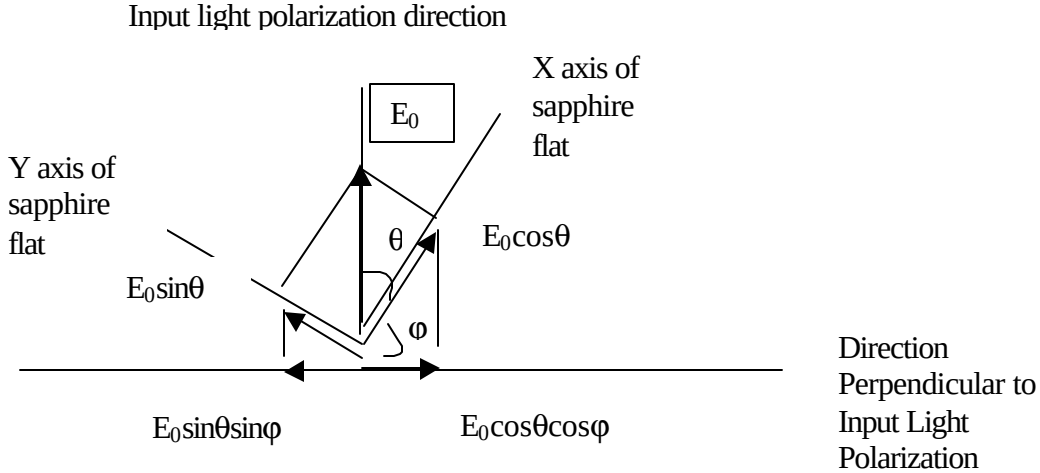

Figure 5. Decomposition of the Input Linearly Polarized Lightwave

If we put another linear polarizer with its transmission direction perpendicular to the original input light polarization direction, and we let the angle between the X axis of sapphire flat and its transmission direction be φ, then the final output will be

$$\vec{E}_{out} = \vec{E}_0 \sin q \sin j + \vec{E}_0 \cos q \cos j \tag{3}$$

where $\vec{E}_{out}$, $\vec{E}_0 \sin q \sin j$ *and* $\vec{E}_0 \cos q \cos j$ are all vectors. If we detect the intensity

$$I = (E_{out})^2 \tag{4}$$

the results will contain the information about d, which is the result of the interference of the two polarizations of the lightwave:

$$\begin{aligned} I_{out} &= (E_0 \sin q \sin j)^2 + (E_0 \cos q \cos j)^2 - 2E_0^2 (\sin q \sin j \cos q \cos j) \cos d \\ &= I_0 (\cos^2 (j + q) + \sin 2q \sin 2j \sin^2 (d/2)) \end{aligned} \tag{5}$$

From equation (3), d is a function of the product $d\Delta n$. When temperature changes, the thickness d of the sapphire flat will change, and $\Delta n = n_o - n_e$ will also change. Therefore, the measured intensity from equation (5) will be a function of temperature. Because the sapphire flat thickness change Δd is:

$$\Delta d = a \, d\Delta T, \tag{6}$$

and d>>Δd, d can be considered as constant. Therefore, the sapphire thickness d' at temperature T is

$$d' = d(1 + a(T - T_0)) \Rightarrow d' = adT + A(cons \tan t) \tag{7}$$

where a is the thermal expansion coefficient for the sapphire material, ΔT is the temperature change, T_0 is room temperature = 25°C, and A= $d - adT_0$ is a constant.. Considering that $\Delta n = n_o - n_e$ is very small approximately 13×10^{-6}/°C (from Saphikon, the sapphire crystal manufacturer), the relation between temperature and the product $d\Delta n$ will be linear, and the temperature relation with the output light intensity (polarization direction perpendicular to input linearly polarized light) will be a squared sinusoidal function as in

$$
\begin{aligned}
I_{out}(T) &= I_0(\cos^2(j+q) + \sin 2q \sin 2j \sin^2(d/2)) \\
&= I_0(\cos^2(j+q) + \sin 2q \sin 2j \sin^2(p\Delta n d'/l)) \\
&= I_0(\cos^2(j+q) + \sin 2q \sin 2j \sin^2(p\Delta n a dT/l) + Ap\Delta n/l)
\end{aligned} \tag{8}
$$

where $Ap\Delta n/l = \Phi$ is a single constant phase. Then

$$
I_{out} = I_0(\cos^2(j+q) + \sin 2q \sin 2j \sin^2(p\Delta n a dT/l) + \Phi) \tag{9}
$$

Since j and q are constant numbers in the experimental setup, I_{out} is only function of temperature.

2.2 Two Beam Interference

In addition to polarization light interference in our system, there is also a multi-beam interference, for either ordinary rays or extraordinary rays. This phenomenon is always present because of the two parallel surfaces of sapphire flat.

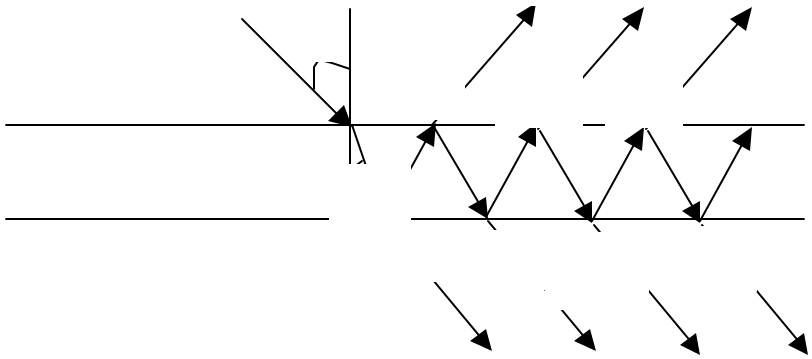

Figure 6. Reflection And Transmission Of A Plane Wave In A Plane Parallel Plate

Generally speaking, when a plane wave is incident upon a plane at angle θ, at the first surface this wave is divided into two waves, one reflected in the direction B_1C_1, and the other transmitted into the plane in the direction B_1D_1. The latter wave is incident on the second surface at angle θ', and is there divided into another two waves, one transmitted in the direction D_1E_1, and the other reflected back into the plate in the direction D_1B_2. If we let A be the amplitude of the electric vector of the incident wave, and r be the reflection coefficient (ratio of reflected and incident amplitude), t be the transmission coefficient (ratio of transmitted and incident amplitudes), and r', t' be the corresponding coefficients for the wave propagate from the plate to the surrounding medium, and utilizing the phase difference between each neighboring transmitted ray (or reflected ray) given by

$$
d = 4pn'h\cos q'/l_0 \tag{10}
$$

where h is the thickness of the plate and l_0 is the wavelength in vacuum, then the complex amplitudes of the waves reflected from the plate are:

$$tt'A,\ tt'r'^2A\exp(i\delta),\ tt'r'^4A\exp(i2\delta),\ \ldots..tt'r'^{2(p-1)}A\exp(i(p-1)\delta),$$

where p is the numbers of transmitted rays. The total transmitted energy will be the square of all these amplitude summations.

For our case, the incident angle θ=0, but there still exists multi-reflection in the sapphire flat. This transmission process can be approximated as a two beam interference problem such that

$$I'_{out} = \left|(tt'A + tt'r'^2 A\exp(i\delta))\right|^2 = (tt'A)^2(1+r'^2+2r'\cos(\delta)) \qquad (11)$$

If $\delta = 4\pi n'h\cos\theta'/\lambda_0 = 2k\pi$, the maximum intensity output is achieved from these two beams, while for $\delta = 4\pi n'h\cos\theta'/\lambda_0 = (2k+1)\pi$, the minimum intensity output is observed from these two beams, where k is a positive integer.

From the discussion in Section 2.2 and Section 2.3, from equation (9) and (11), the total intensity will be :

$$I_{out}+I'_{out} = I_0(\cos^2(\psi+\theta) + \sin 2\theta \sin 2\psi \sin^2(\pi\Delta n a dT/\lambda) + \Phi) + (tt'A)^2(1+r'^2+2r'\cos(\delta)) \qquad (12)$$

This is the relation which governs the observed intensity versus change in the environmental temperature for the sensor head design used in this segment of the experimentation.

2. Experimental Procedure

The system used in this phase of the experimentation is shown schematically in Figure 7. Linearly polarized light from a helium neon laser is directed into the temperature sensing probe (the birefringent sapphire flat), where the light's status of polarization (SOP) will be affected by temperature. The output optical signal containing the temperature information is directed into the detecting unit which converts the optical signal into electrical signal (voltage). After processing the input signal, the temperature can be determined directly from the voltage signal and displayed on the display unit. The temperature sensing probe and detecting unit will be described below in detail.

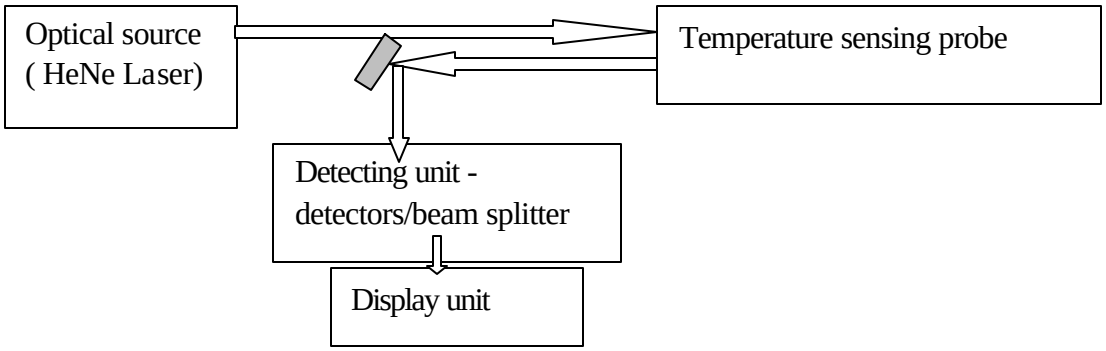

Figure 7. Schematic Of The Polarimetric Sensor System For High Temperature

2.1 Temperature Sensing Probe Design

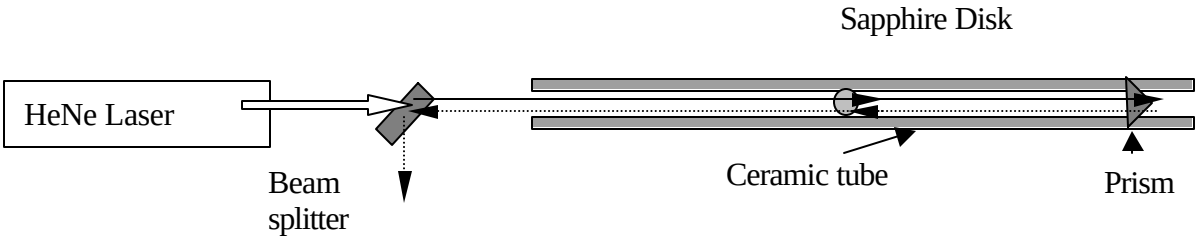

Figure 8. Schematic of the Temperature Sensing Probe Design

The schematic operation of the temperature sensing probe is shown in Figure 8. Because of the harsh working environment for this sensor in the coal gas application, the sensing element will need to be protected from being damaged or polluted. A sapphire tube will be used to protect the sapphire flat from fouling as shown in Figure 8. The prism shown is used to reflect the light back. This design minimizes the probe size. Outside the probe, only laser source and one beam splitter are needed. The beam splitter reflects the output light from the probe to detecting unit.

In order to test if the sapphire flat can work as the sensing element, the experiment setup used for this phase of the experimentation is shown in Figure 9. This is a prototype of the temperature sensing probe which could be used in the gasifier, and can be integrated together with the sapphire outer tube to form the desired sensing probe for practical usage. In Figure 9, the sapphire plate is put directly in the furnace so the temperature can be controlled easily for calibration.

2.2 Detecting Unit

The detecting unit setup is shown in Figure 10. In general, the phase values generated by the birefringent retarder (sapphire flat) can be any positive real number, so the light output from the probe will be elliptically polarized light, A polarizing beam splitter (PBS) is used to split elliptically polarized light into two orthogonal, linearly polarized components, as shown in Figure 11. As shown in this Figure, p-polarized light is transmitted, while s-polarized light is reflected, both with negligible absorption by the

beam splitter. Two separate detectors (D1 and D2) were used to detect these two components and the signals are transmitted along two channels. By combining these two channels of information, self-calibration can be easily achieved, which eliminates the influence of the laser power fluctuation. This is a significant advantage of this type of design.

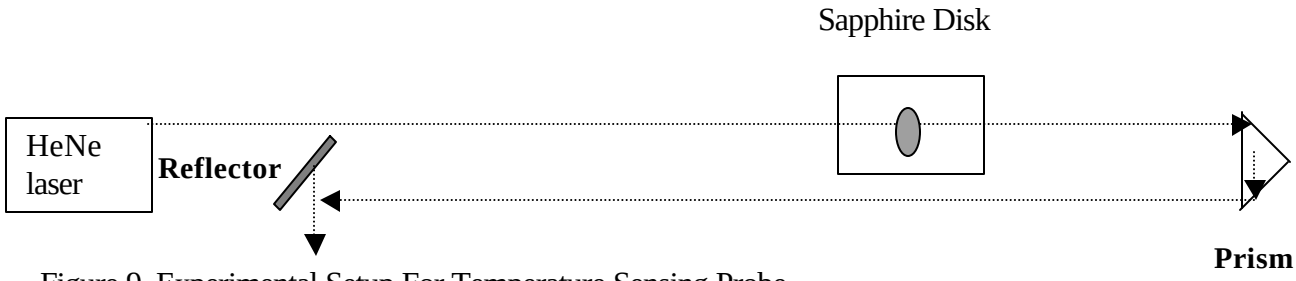

Figure 9. Experimental Setup For Temperature Sensing Probe

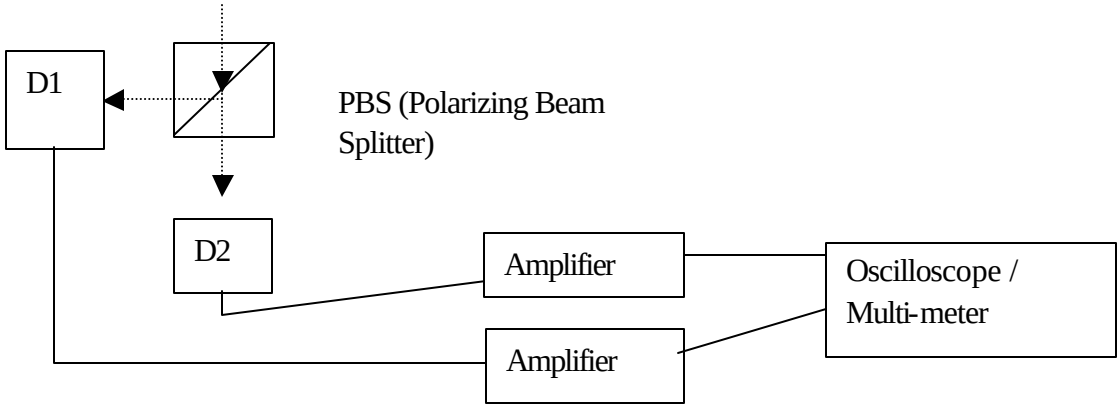

Figure 10. Schematic of the Detection Unit

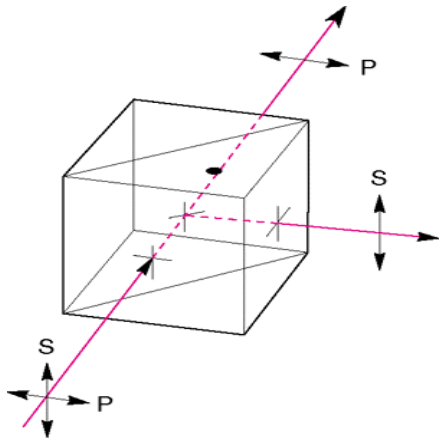

Figure 11. Schematic of the Polarizing Beam Splitter

The two detectors (D1 and D2) which were used were silicon photodiodes. These photodiodes are semiconductor light sensors that generate a current when the P-N junction in the semiconductor is illuminated by light. Current signals from the two channels are input into the two impedance amplifiers separately. Output signals from the amplifiers are electric voltage signals which are be easily detected by simple multimeters or oscilloscopes.

4. Experimental Results

A photograph of the actual experimental setup used to measure the temperature coefficient of the birefringence of single crystal sapphire is shown in Figures 12 a, b, and c.

Figure 12 (a). Photograph of the Experimental Setup for Measurement of the Temperature Coefficient of Birefringence of Single Crystal Sapphire

The furnace used for this set of experiments was a Thermolyne box type front-loading 1200° C maximum temperature capability furnace. A K-type (chromel-alumel) thermocouple was used to monitor the temperature immediately adjacent to the single crystal sapphire plate as shown in Figure 12 b.

Figure 12 (b). Photograph Of The Single Crystal Sapphire Plate Inside The Furnace

As shown in Figure 12 b., the single crystal sapphire plate was placed in a piece of low-density, alumino-silicate refractory brick. A slot the width of the sapphire plate was cut into the refractory brick to hold the specimen during heating. In this manner, no refractory cement had to be used which could influence the results. The thermocouple was placed close to the specimen. A hole was drilled from the back of the furnace. A similar size hole was aligned and drilled through the front of the furnace such that the laser beam directed through the hole in the rear of the furnace would pass through the single crystal sapphire plate and exit the front of the furnace unobstructed. The system with the door closed and the laser beam in operation is shown in Figure 12 c. The laser beam can be clearly seen exiting the furnace, being reflected at the 45/45 prism and contacting the detected heads.

The helium neon laser (wavelength $l = 632.8nm$) is used directly as the light source. The output from the laser is already linearly polarized because the output mirror in the laser cavity is tilted by an angle corresponding to the Brewster angle. One of the sapphire flat's optical principal axes (X axis or Y axis) is aligned at 45^o relative to the light polarization direction, i.e. $q = 45^o$. By using PBS, the two orthogonal components of the output light are separated into two directions and measured individually. During the testing process, the temperature was either increased from room temperature (25^oC) to 1200^oC, which was the temperature maximum of the furnace used, or cooling down from 1200^oC to room temperature. In all experiments, the temperature was also measured by using a thermocouple (K type).

Figure 12 c. Photograph Of The Experimental Setup In Operation During Testing

The sapphire flat used in the setup was a disk, with thickness d=1.05mm, diameter $\Phi = 25.36mm$. The detectors used were silicon photodiodes (from UDT). The impedance amplifiers (from Oriel) were used to transform the current signal into a voltage signal with a gain of 10^4(V/A). Two multimeters were used to measured the voltage signals. Many experimental runs were performed; one typical result is shown in Figure 13., where the voltage was recorded every 10^oC.

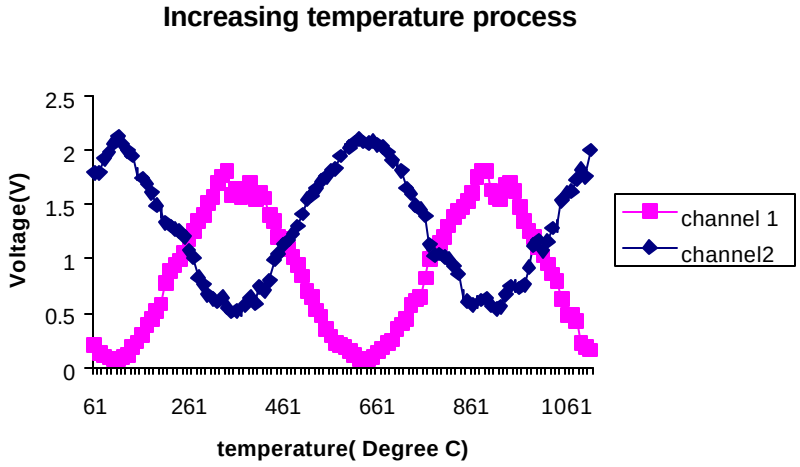

(a)

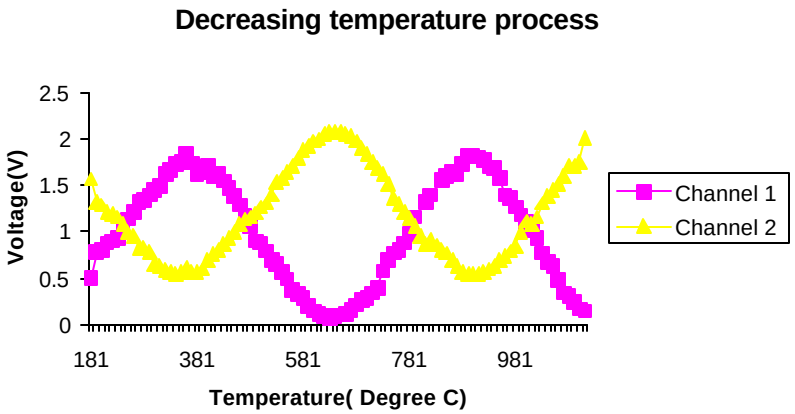

(b)

Fig 13, Experimental Results: Two Channel Signals versus Temperature.
(a) Increasing Temperature From 61 ^{O}C To 1111 ^{O}C;
(b) Decreasing Temperature From 1111 ^{O}C To 181 ^{O}C.

5. Discussion of the Experimental Results

Based on the theoretical analysis in Section 2, equation (9) predicts that the voltage signals should be a squared sinusoidal function of temperature, which is clearly the result obtained as shown in Figure 13. Due to the thickness of the sapphire disk we used, there were approximately two periods shown for the temperature change in the range from 61^{o}C to 1111^{o}C. Several experimental runs are also shown in Figure 14.

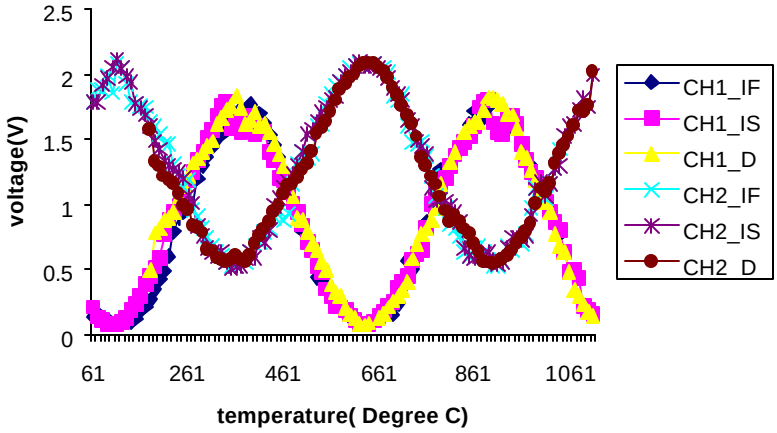

Figure 14. Experimental Results Of The Temperature Sensing System. CH1_IF: Channel1 signal for increasing temperature faster; CH1_IS: Channel1 signal for increasing temperature slower; CH1_D: Channel1 signal for decreasing temperature; CH2_IF: Channel2 signal for increasing temperature faster; CH2_IS: Channel2 signal for increasing temperature slower; CH2_D: Channel2 signal for decreasing temperature.

In this set of experimentation, increasing temperature slowly or quickly, or deceasing temperature slowly or quickly had very little effect on the response of the sensor system. What small differences are present can be explained by the differences in response time of the sapphire plate as compared to the thermocouple which was used as the reference. Figure 14 shows the repeatability and stability of this system during these cycling tests.

There are, however, some ripples along the curves shown in Figure 14, especially at the peaks and valleys of the sinusoid. These are caused by the two beam interference generated by the two parallel surfaces of the sapphire disc. This interference phenomenon was analyzed in Section 2.3 in detail. If we align the disc with one of its principle axis, for example the X axis, parallel to polarized direction of input linear polarization light, i.e. $q = 0$, there will be no light component along Y axis, and the polarization light interference is therefore eliminated.

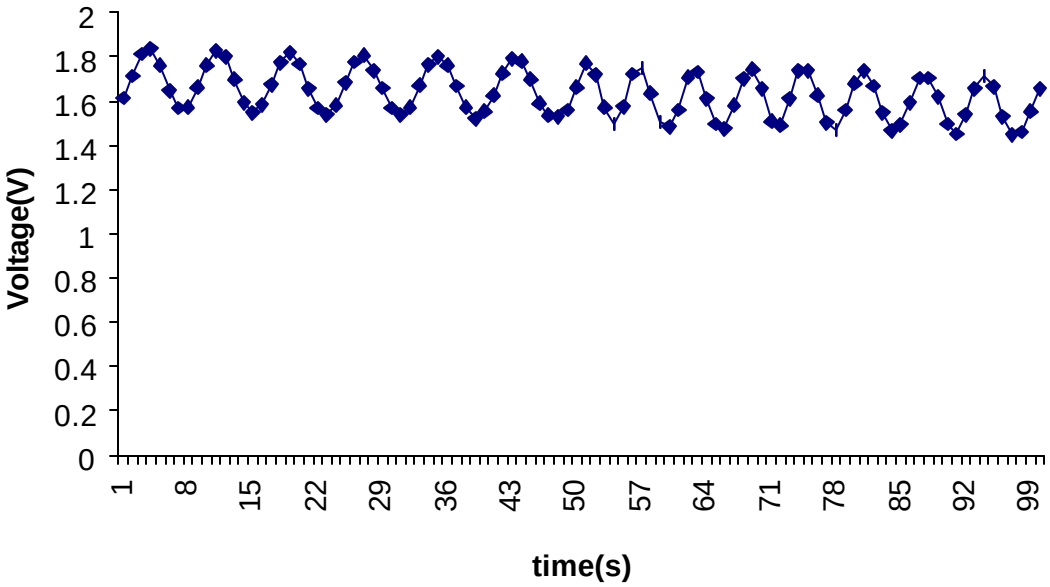

Fig15. Voltage Signal Vs. Time During Temperature Increasing Process

Figure 15 was recorded by a computer with the data plotted as a function of time instead of temperature. The data were collected every 10 seconds, while the furnace was heated from 790 ^{o}C to the maximum. We can not see the effect of the polarized light interference in this set of data, only the two-beam interference. The two beam interference is always there for both channels, because of the low reflectivity of the sapphire disc surface. The two beam interference is about one order of magnitude less than the polarization light interference. Because all the data are obtained in a dynamic process, in the peak and valley regions it is easy to observe the two beam interference effect, while in the other regions it is swamped by the polarization interference. The two beam interference is not obvious in the rising and falling regions of the curve, but it still exists. In the future work this two beam interference signal will be minimized by polishing a certain angle between two surfaces. On the other hand, equation (11) also shows that the two beam interference is a function of temperature, such that careful

calibration of the system may eliminate the need for precise angle polishing of the sapphire plate. This will be investigated for the next reporting period as well.

To evaluate the temperature measurement accuracy, as shown in Figure 13 (a) channel 1, $j = q = p/4$, and equation (12) is simplified into equation (14) which resulted in the relation that the light intensity is a squared sinusoidal function of temperature(regardless of two beam interference part). The temperature can be obtained by solving equation (14):

$$I_{out} = I_0 \sin^2((p\Delta n a dT / l) + \Phi)) = I_0 \sin^2(BT + C) \qquad (14)$$

where B and C are approximated as constant numbers. By putting I_{out} numbers into equation (14), I_0, B and C are determined, then T can be calculated individually by each I_{out}. The fitting curve and original data is shown in Figure16, the fitting curve function is:

$$I_{out} = 1.81\sin^2(0.006T - 0.6672) \qquad (15)$$

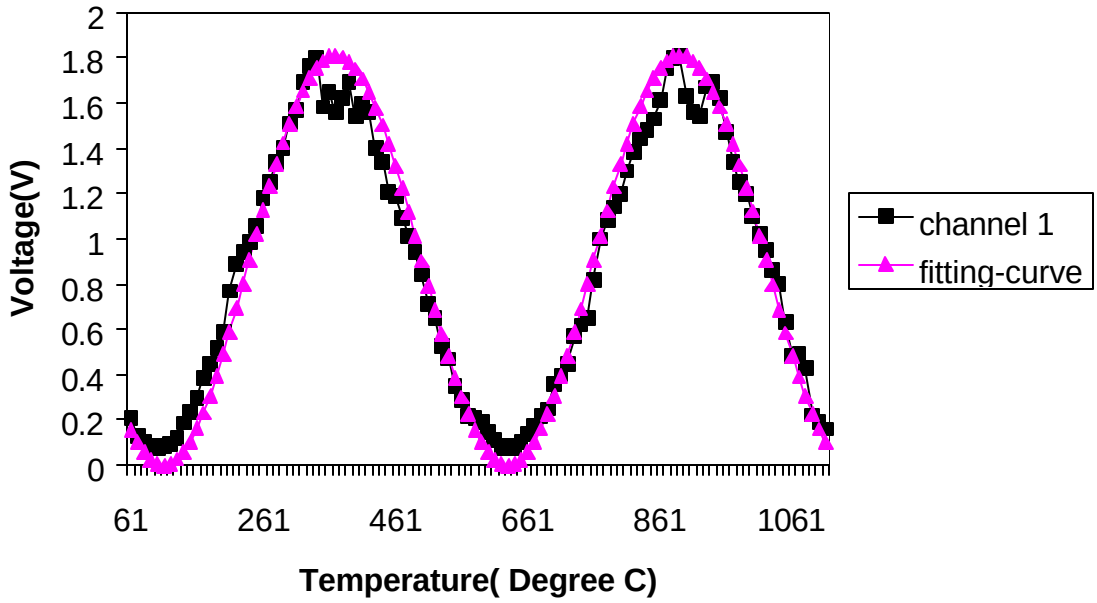

Figure 16. Squared Sinusoidal Function Curve Fit of Channel One Data

Based on the data from channel 1, and by inversing equation (15), the temperature results from the polarimetric sensor system can be calculated. The results of this operation are plotted in Figure 17 along with the thermocouple data.

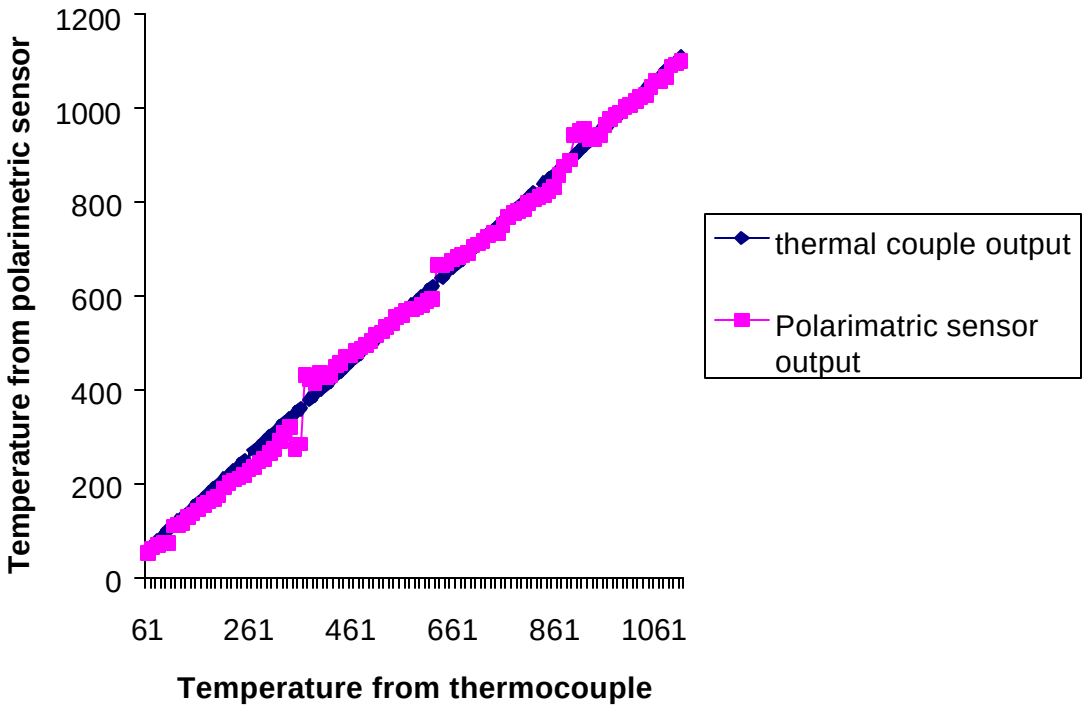

Figure 17. Polarimetric Sensor Results As Compared With Thermocouple Results

Figure 18 shows the difference between the thermal couple output and the polarimetric sensor output. We can see that a relatively large difference occurs at the peak and valley regions of the squared sinusoidal function, which is remarkably affected by the two beam interference as discussed in Section 2.3. For the testing temperature range, most of the difference is under 30 ^{o}C, and at higher temperature, the differences are even smaller for this fitting curve.

Because the response of polarimetric sensor is a periodic function, the output voltage does not correspond to the temperature by one-to-one relation. In future experiments, a thinner sapphire flat will be used to restrict the size to one quarter of a period for the proposed temperature measurment range. Then the temperature and voltage signal will be a one-to one relation. By designing the polarimetric sensor working position and working range of the response function (squared sinusoidal function), the peak and valley effect will be greatly reduced, which means the difference between the thermocouple measurement results and the polarimetric sensor measurement results will be minimized. The effect of response time of the thermocouple in contrast to the sapphire flat will also be investigated in the next reporting period to determine the magnitude of the contribution on the sensor signal.

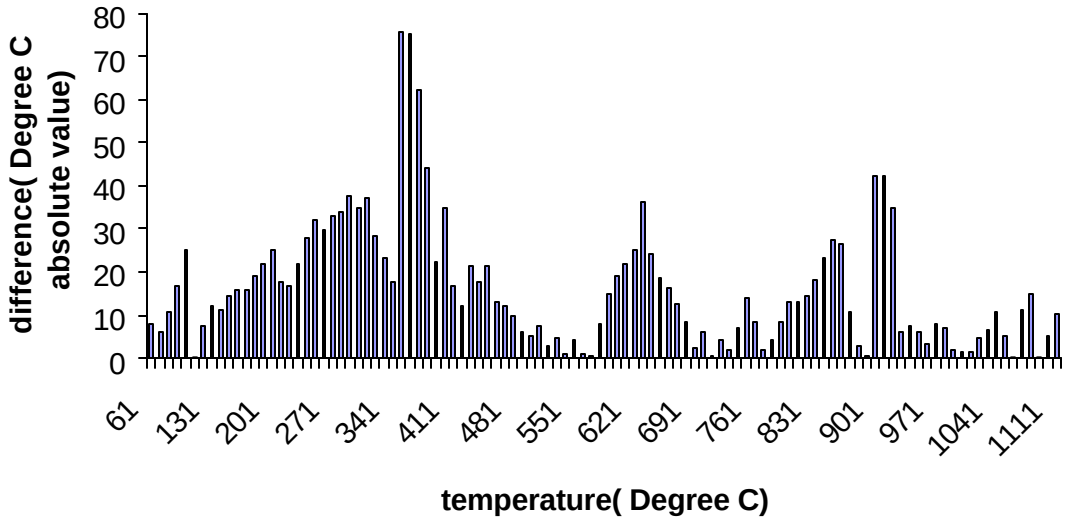

Fig 18. Difference Between Thermal Couple Results And Polarimetric Sensor Results

6. Self-Calibration Principle Discussion

One advantage of the polarimetric sensor system is the potential for self-calibration. The detecting unit detects two channels simultaneously as shown in Figure 10. These signals are two linearly polarized light vectors with polarization direction perpendicular to each other. The output of channel one follows equation (14), and because of energy conservation, the output of channel two follows equation(16) (regardless of the two beam interference):

$$I_{out-2} = I_0(\sin^2(j+q) - \sin 2q \sin 2j \sin^2((p\Delta nadT / l) + \Phi)) \qquad (16)$$

which also contains information of the temperature and input laser intensity I_0.

Usually, input laser intensity I_0 is not stable, and one channel signal will be affected by I_0 directly. If we combine the signals from channel one and channel two by some method to cancel it, the final signal will be only affected by temperature. This will be a significant advantage because it will offer flexibility on light source used , and we can even change the laser source without recalibrating the whole system. In reality, the response curve to light intensity of the two detectors will never be the same, some factors will be necessary to modify equation (14) and equation (16) to eliminate laser intensity I_0, equation (16) is modified into equation (17) , and in our experiments, $q = j = p/4$,to be consist with equation (14):

$$\begin{aligned} I_{out-2} &= I_0(E\sin^2(j+q) - F\sin 2q \sin 2j \sin^2((p\Delta nadT / l) + \Phi)) \\ &= I_0(E - F\sin^2(BT + C)) \end{aligned} \qquad (17)$$

where E and F are constant for a selected detector and can be determined by calibration. From equation (14) and (17) we obtain:

$$\sin^2(BT + C) = (E - (I_{out-2} / I_{out})) / F \,. \qquad (18)$$

In the experiment shown in Figure 13(a), B=0.006, C=-0.6672, E=2.13, F=1.61, and the temperature values from the polarimetric sensor after self-calibration is shown in Figure 19, and compared with thermocouple results.

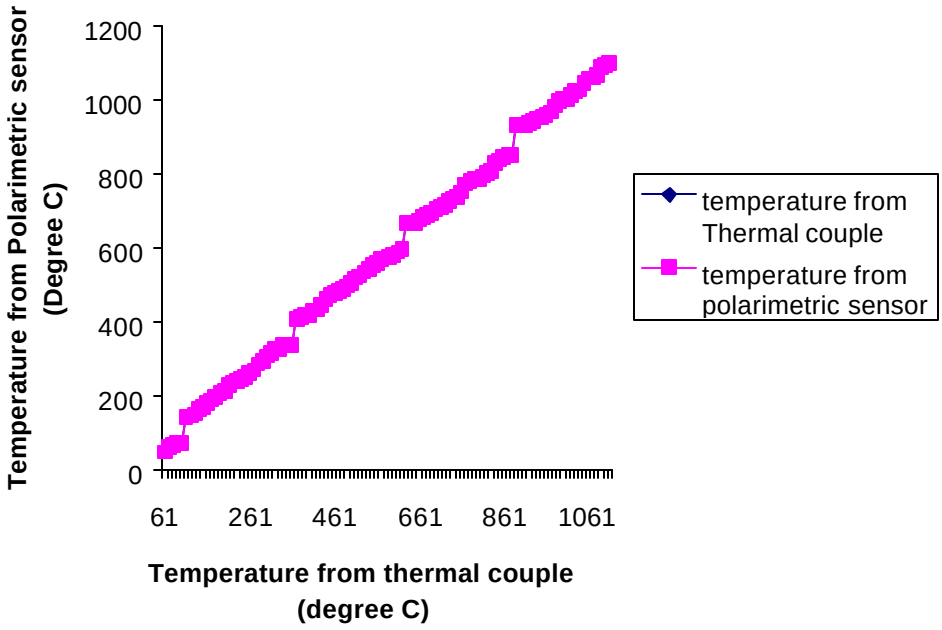

(a)

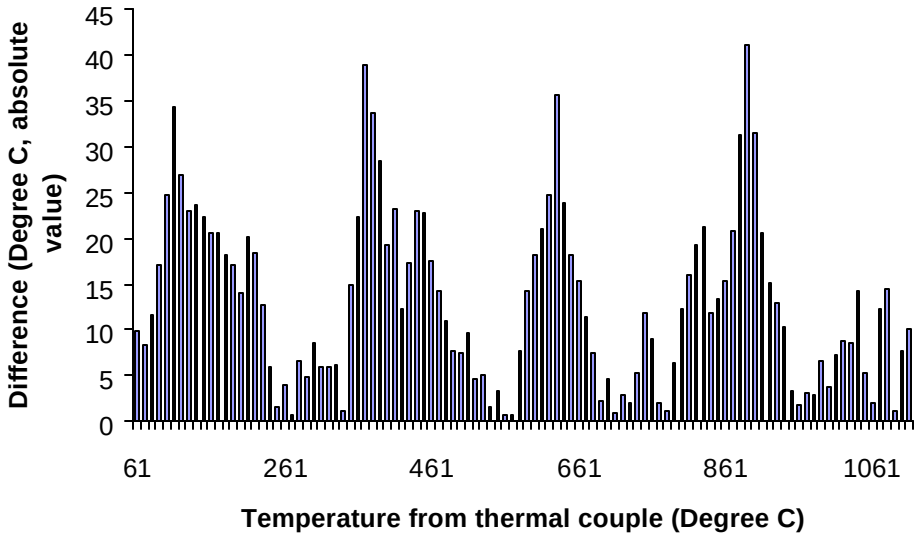

(b)

Figure 19. Temperature Values After Self-Calibration (a) Temperature of the Polarimatric Sensor versus Thermocouple Output, (b) Difference versus thermocouple temperature

After eliminating the effect of laser intensity, the difference between the thermal couple and polarimetric sensor are greatly reduced (compare Figure19(b) and Figure (18)). The largest differences are still centered on the peaks or valleys of response curve. These differences will be further minimized in the future experimentation.

5. Future Instrumentation System Development And Testing Evaluation

Based on the sensor configuration and self-calibration method discussed above, a prototype instrumentation system will be developed for the future system testing and evaluation. Several temperature probe assemblies will be fabricated, a practical optoelectronics support system comprising an optical source (such as helium neon laser, or laser diode), photodiode detector, polarization dependent beam splitter (PBS), impedance amplifier, and display box will be developed. The output of the impedance amplifier will interface with the computer through an analog-to digital converter, a program for calculation of temperature from the optoelectronic system output will be written in either Visual BASIC or LabVIEW; a graphical user interface (GUI) will be used to display the data for inspection; and the data will also be stored on hard disk for further analysis.

SECTION II. Corrosion Testing in Coal Slag Environment

1. Experimental Procedure for Corrosion Testing in Coal Slag

The equipment and procedures to perform simulated testing of the corrosion resistance of the single crystal sapphire fiber optic waveguide in coal-gas environments is described below. This testing has been performed in collaboration with inputs from Dynegy, who provided the coal slag samples for testing from their Wabash River Coal Gasification Facility.

An apparatus for studying the corrosion resistance of single crystal sapphire was constructed at Virginia Tech. A 1600° C tube furnace was used which was fitted with a 2.54cm O.D. high purity alumina tube. The tube was purchased in sufficient length such that the ends of the tube extended outside the ends of the furnace. The alumina tube was sealed on both ends to 0.63cm I.D. plastic tubing. The flow rate of gases in the tube was fixed at 30 ml/min. Compressed air has been used in the initial phase of the corrosion testing. Single crystal sapphire plates were purchased from commercial vendors and were cut into samples approximately 0.5cm x 0.5cm. The samples were cleaned and placed in a high purity alumina sample holder (boat). Dense, polycrystalline alumina samples were prepared and placed in the boats as a control and comparison. The alumina boats were filled with coal slag from the Wabash River Coal Gasification facility. The boats were placed in the tube furnace and heated for various periods of time up to 48hrs, at temperatures up to 1500° C.

The samples after the designed heat treatment in the coal slag were removed and cooled. The samples were removed by fracturing the coal slag (and alumina boat) and cutting

with a diamond saw if necessary. Great care was taken to ensure that the coal slag region around the single crystal sapphire plate was left undisturbed. The single crystal sapphire plate with the coal slag still intact on the upper and lower surfaces was polished to expose the end view of the plate. The polished samples were examined for morphological changes across the coal slag/sapphire interface by scanning electron microscopy (SEM). The composition of the interface region was mapped by EDAX elemental analysis.

The results of this experimentation showed that the single crystal sapphire plates underwent almost no detectable corrosion. Based upon the positive results of the immersion testing of the single crystal sapphire plate results, a second apparatus was constructed. For this set of tests, optical quality single crystal sapphire fibers were purchased from a commercial vendor. A dense, polycrystalline boat was cut with a diamond saw to produce a thin slit approximately 500 microns on each side of the boat. The photo of the apparatus constructed for the sapphire fiber corrosion testing is shown in Figure 20. The schematic layout of the system is shown in Figure 21.

Figure 20. Photograph of the Corrosion Testing Apparatus

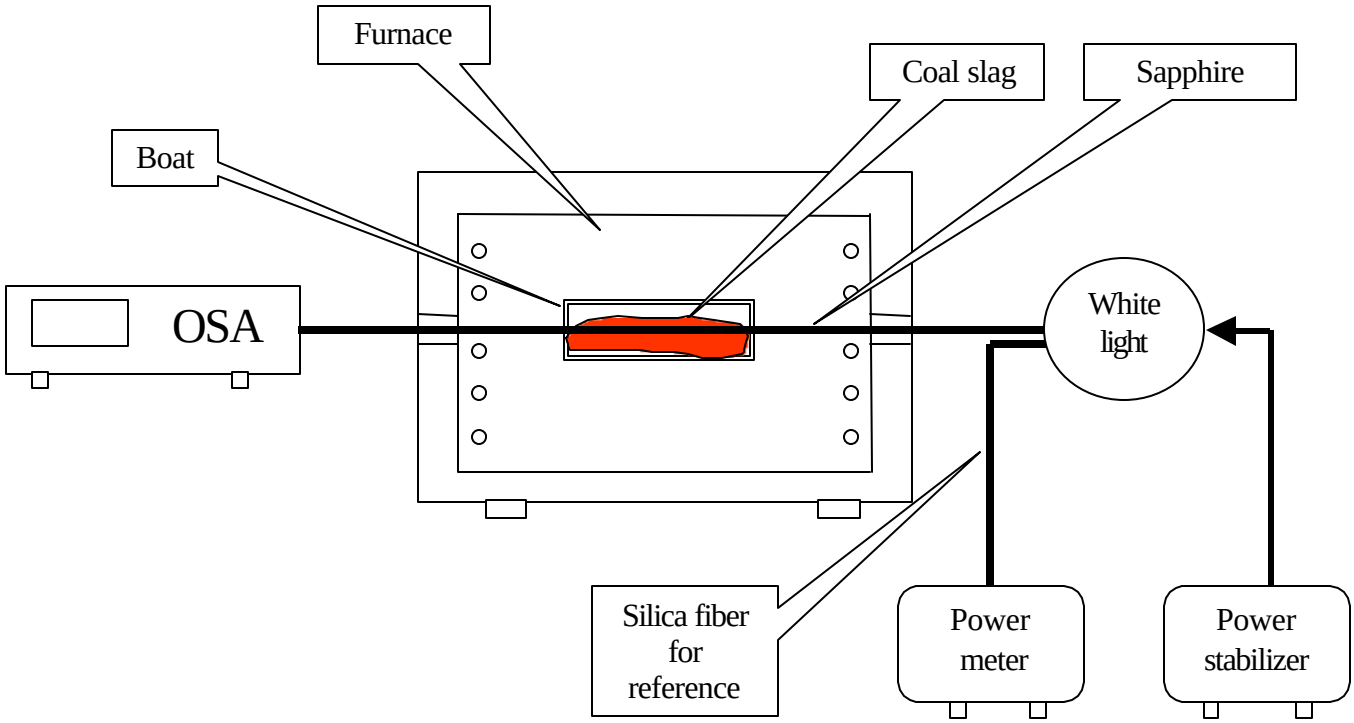

Figure 21. Schematic Layout of the Single Crystal Sapphire Fiber Experimental Setup

A single crystal sapphire fiber was inserted directly into the slits in the alumina boat. The boat with the single crystal sapphire fiber was filled with coal slag and was inserted into the box furnace. The box furnace had been drilled with appropriate size holes to allow the passage of the fiber through the walls of the furnace. A white light source was used, which was connected to the sapphire fiber through two couplers (please refer to Figure 20.). A reference silica fiber was connected to one of the couplers to serve as a reference channel to detect possible changes in the source power. The other end of the sapphire fiber was connected directly to the analyzer. An Optical Spectrum Analyzer was used to monitor the attenuation of the white light signal in the range form 400 to 1700nm, as well as the total output power. The alumina boat was filled with slag from the Wabash River Facility. The system was heated to 1450° C and the optical attenuation as a function of wavelength was monitored.

2. Results of Coal Slag Corrosion Testing

The single crystal sapphire fibers have been immersed in the coal slag from the Wabash River Facility at 1450° C for 2 months. The spectral output from the sapphire fiber has been monitored periodically throughout the corrosion exposure period using an optical spectrum analyzer (OSA). The intensity versus wavelength has been monitored in the range from approximately 400 to 1700 nm. The total power received from the fiber has also been monitored. The signal from the sapphire fiber has remained essentially constant throughout the testing period as shown in Figure 22.

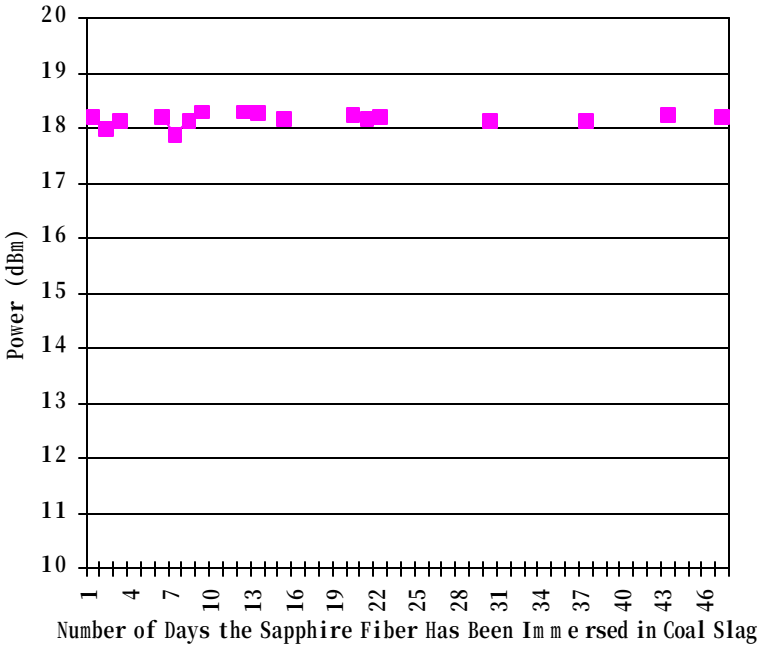

Figure 22. Transmitted Power versus Number of Days Immersed in Coal Slag

A significant portion of the total power received by the OSA through the sapphire fiber is the result of the blackbody emission as well as the white light source. At such high temperatures as 1450° C, the intensity of the blackbody radiation emitted is quite high. This constitutes a significant portion of the signal being monitored. After exposure at 1450° C for the appropriate period of time, the signal from the system will be monitored during the cooling of the fiber. This will allow characterization of the contribution of the blackbody radiation to the signal and to allow measurement of the transmitted power from the white light source at room temperature. These data will be presented in the next reporting period.

Section III. Site Visit to the Wabash River Coal Gasification Facility

During this reporting period, Dr. May and Dr. Pickrell visited the Wabash River Coal Gasification Facility. The purpose of this visit was to discuss the operational requirements for the sensor including the gasifier environment, feed through restrictions and interfacing requirements, and tour the facility. During this visit, a tour of the inside of the gasifier unit was conducted (units were down for maintenance) by the personnel at the Wabash River Facility. Requirements for temperature of operation, position in the gasifier, stages to be instrumented in the gasifier, slagging conditions at the temperature measurement points, length into hot zone, length of refractory, location of electronics,

etc. were discussed. This visit was extremely helpful in conceptualizing the requirements for the entire system.

Conclusions:

Investigation of the birefringence based single crystal sapphire sensor technique to measure temperatures of the exposed sapphire flat has indicated that this is a viable method to measure temperature. Comparison of the data from thermocouple measurements and the birefringence based sensor showed the two methods were in good agreement. The single crystal sapphire fiber exhibits good corrosion resistance when immersed in the coal slag at 1450° C. The total signal transmission, which included components from the white light source as well as blackbody radiation, remained constant with exposure time in the coal slag at 1450° C up through 50 days of exposure (the test is still in progress). The data generated to date for the sapphire temperature sensor development looks promising.